Supporting Information

Organoiodine Functionality Bearing Resists for Electron-Beam and Helium Ion Beam Lithography: Complex and Sub-16 nm Patterning

Midathala Yogesh,[a,] Mohamad. G. Moinuddin,[b] Manvendra Chauhan,[b] Satinder K. Sharma,[b] Subrata Ghosh,[a,*] Kenneth E. Gonsalves[a,*]

[a]School of Basic Sciences, Indian Institute of Technology Mandi, H.P. 175005, India.

[b]School Computing and Electrical Engineering, Indian Institute of Technology Mandi, H.P. 175005, India.

*e-mail: subrata@iitmandi.ac.in, kenneth@iitmandi.ac.in

*Phone: +91-1905267069

Procedure for the synthesis of MAPDST (1):

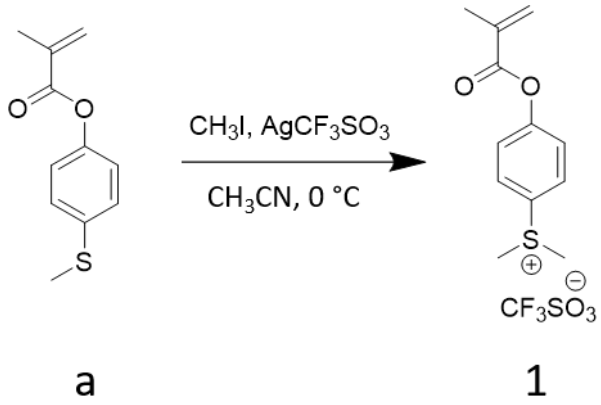

a 1

Scheme: S1 Synthesis of MAPDST

MAPDST was synthesized following a literature method.[1] To a stirred solution of 4-(methylthio)phenyl methacrylate (**a**) (8g, 0.03 mol) and silver trifluoromethanesulfonate (9.8 g, 0.03 mol) in acetonitrile (40 ml) was dropwise added methyl iodide (5.4g, 0.03 mol) (20 ml) at 0 ºC under nitrogen atmosphere in dark condition. The resulting solution was stirred for 3 hr at 0 ºC. After completion of reaction, the reaction mixture was filtered and washed with acetonitrile. The organic layer was concentrated using rotary evaporator and the obtained residue was recrystallized from hot THF. The pure product was isolated as white crystals. Yield: 9.4 g (65 %). ^{1}H NMR (500 MHz, DMSO-d_6): δH = 8.15 (2H, d, *J* = 8.9 Hz, ArH), 7.58 (2H, d, *J* = 8.9 Hz, ArH), 6.33 (1H, s, C=CH), 5.97 (1H, s, C=CH), 3.27 (6H, s, $S(CH_3)_2$), 2.01 (3H, s, CH_3 aliphatic). IR absorption: ν_{max}/cm^{-1} 3032 and 2922 (CH), 1732 (C=O), 1641 and 1577 (C=C), 1281 and 1249 (CF_3).

Procedure for the Synthesis of 2,4,6-Triiodophenyl Methacrylate (2):

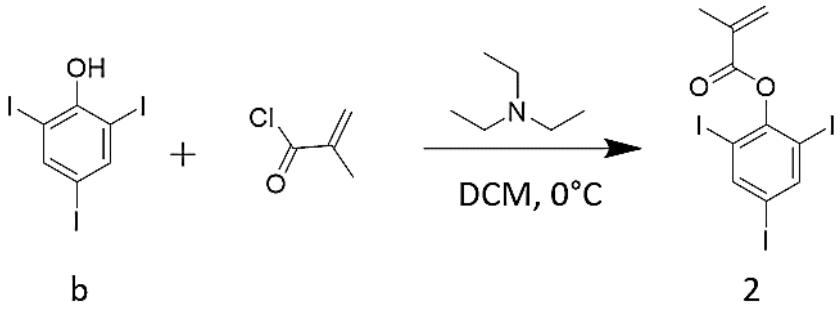

b 2

Scheme S2: Synthesis of TIPMA

2,4,6-Triiodophenyl methacrylate was synthesized following a literature method.[2] 2,4,6 Triiodophenol (**b**) (6g, 0.012 mol) was dissolved in dichloromethane (40 ml) in the presence of triethylamine (1.93 g, 0.019 mol) under nitrogen atmosphere. The resulting solution was cooled to ~0 °C using an ice bath, and methacryloyl chloride (1.59g, 0.015mol) was slowly added into it under stirring condition. The reaction mixture was left for stirring overnight and the resulting precipitate was separated through filtration. The filtrate was washed with water

and dried over Na_2SO_4 followed by evaporation of organic solvent on a rota-evaporator. The crude product was purified using column chromatography (6-10% of ethyl acetate in hexane as eluent) which yielded pure product as white solid. Yield: 5.4g, (78%). ^{1}H NMR (500 MHz, $CDCl_3$): δH, 8.08 (s, 2H, ArH), 6.46 (s, 1H, C=CH), 5.85 (s, 1H, C=CH), 2.11 (s, 3H, CH_3). IR absorption: ν_{max}/cm^{-1} 3051 and 2954 (CH), 1725(C=O), 1634 (C=C), 631(C-I).

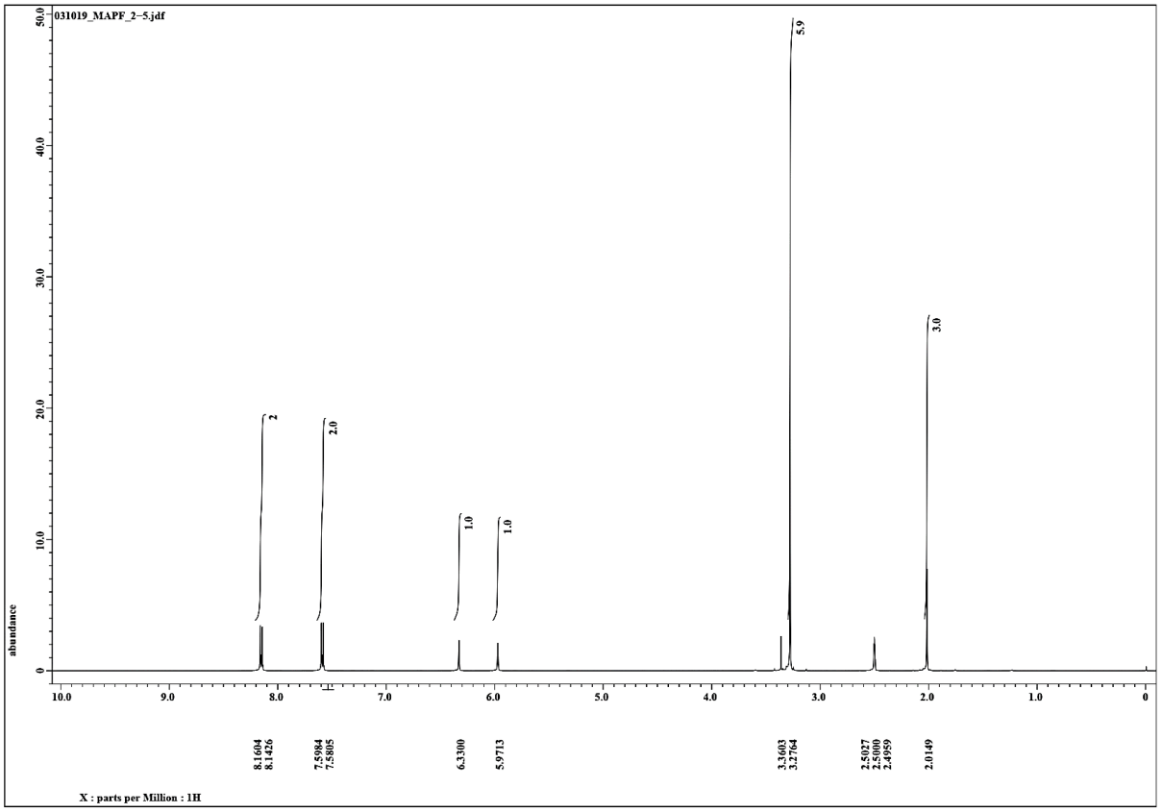

Figure S1: ^{1}H NMR spectrum of 4-(methacryloyloxy)phenyl dimethylsulfonium triflate (MAPDST)

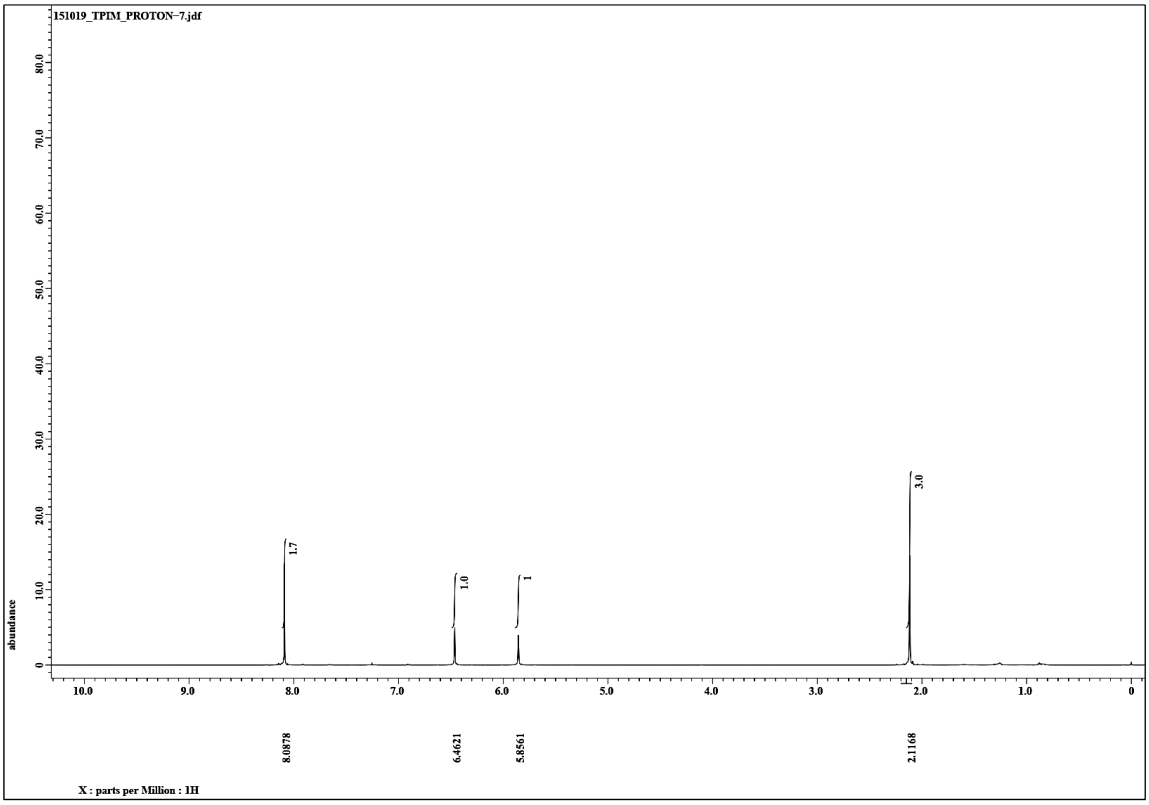

Figure S2: ^{1}H NMR spectrum of 2,4,6-Triiodophenyl methacrylate (TIPMA)

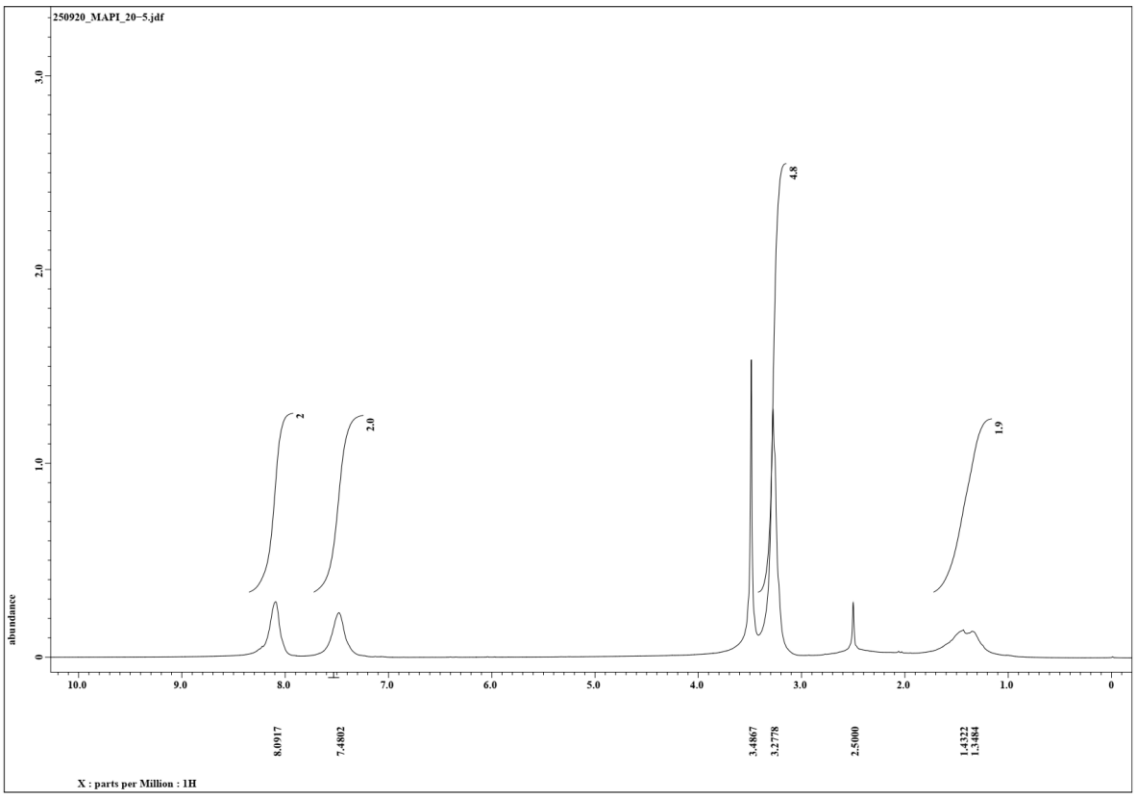

Figure S3: ^{1}H NMR spectrum of polymer **3a**

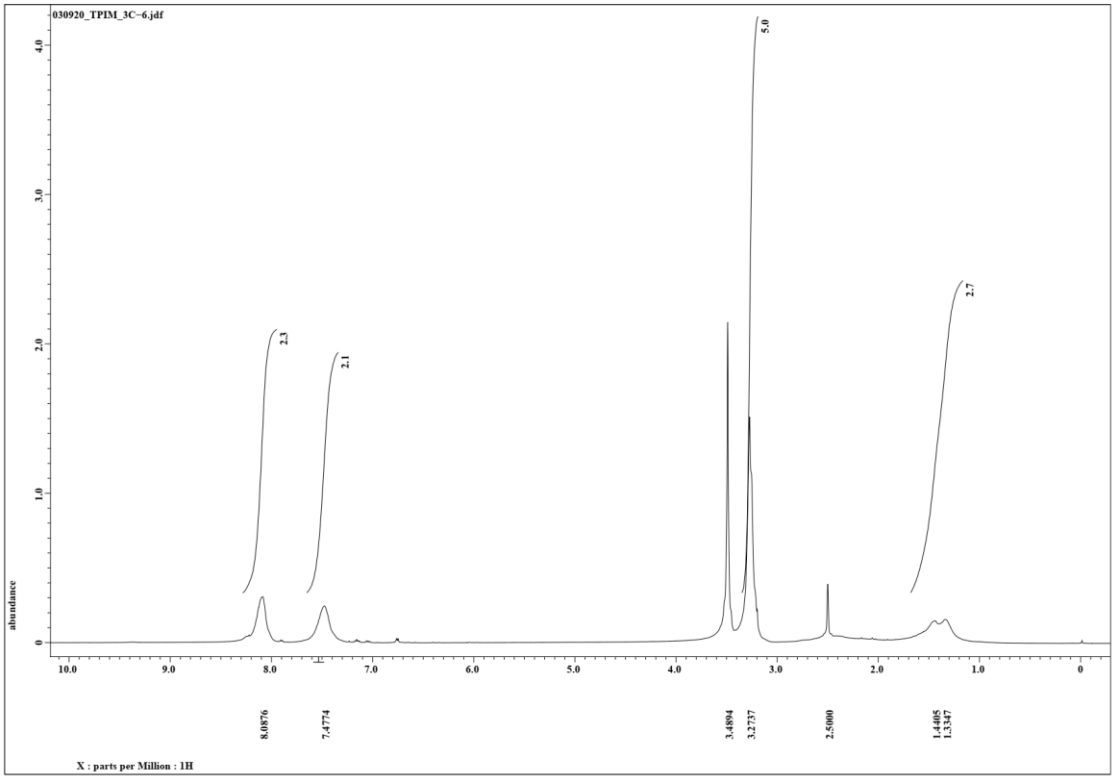

Figure S4: ^{1}H NMR spectrum of polymer **3b**

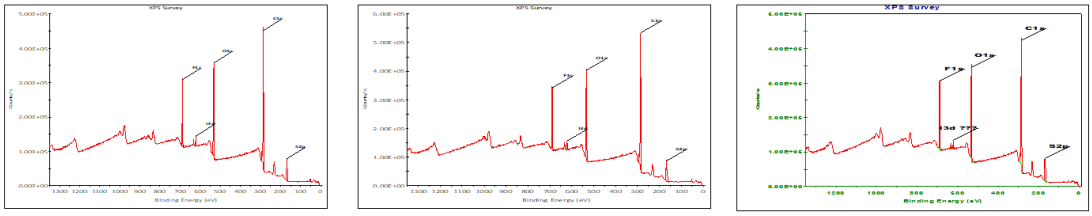

Name	Peak BE	FWHM eV	Area (P) CPS.eV	Weight %
C1s	285.48	1.8	171602.56	50.55
O1s	532.47	2.86	124715.97	20.25
S2p	168.54	3.98	45296.35	17.63
F1s	688.48	1.88	62934.44	9.7
I3d	621.24	1.27	19978.01	1.88

Name	Peak BE	FWHM eV	Area (P) CPS.eV	Weight %
C1s	285.52	1.77	192406.99	50.9
O1s	532.54	1.88	138980.64	20.26
S2p	168.64	4.02	49512.49	17.31
F1s	688.53	1.85	68858.66	9.53
I3d	621.27	1.35	23543.79	1.99

Name	Peak BE	FWHM eV	Area (P) CPS.eV	Weight %
C1s	285.49	1.81	155969.69	45.38
O1s	532.21	1.97	133202.61	21.35
S2p	168.36	3.81	47795.99	18.37
F1s	688.4	1.84	85893.95	13.08
I3d	621.12	1.35	19613.02	1.82

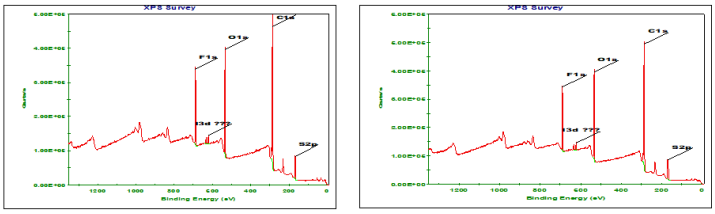

Name	Peak BE	FWHM eV	Area (P) CPS.eV	Weight %
C1s	285.59	1.8	175074.72	46.02
O1s	532.32	1.94	147953.12	21.43
S2p	168.4	3.81	51790.57	17.98
F1s	688.51	1.82	92558.95	12.73
I3d	621.25	1.31	21816.11	1.83

Name	Peak BE	FWHM eV	Area (P) CPS.eV	Weight %
C1s	285.68	1.78	177221.06	46.09
O1s	532.42	1.58	148810.51	21.32
S2p	168.56	3.83	51945.64	17.85
F1s	688.59	1.83	94418.37	12.85
I3d	621.32	1.29	22823.25	1.9

Figure S5: XPS spectrum of polymer **3a**

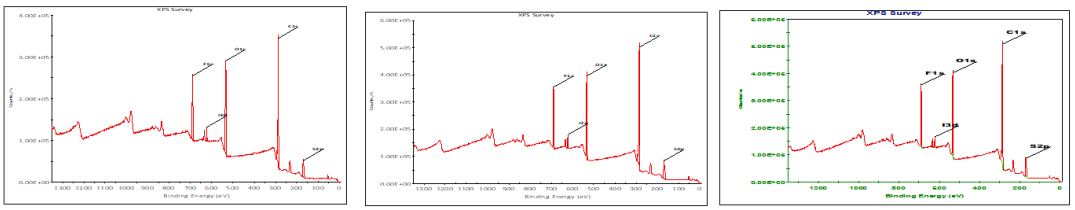

Name	Peak BE	FWHM eV	Area (P) CPS.eV	Weight %
C1s	285.72	1.72	135367.07	51.67
O1s	532.79	1.9	91735.16	19.3
S2p	168.88	4.03	34654.12	17.48
F1s	688.76	1.86	43086.58	8.61
I3d	621.52	1.24	24174.64	2.95

Name	Peak BE	FWHM eV	Area (P) CPS.eV	Weight %
C1s	285.58	1.74	193313.67	50.79
O1s	532.62	2.88	136511.61	19.77
S2p	168.69	4.01	49590.19	17.22
F1s	688.6	1.87	67641.78	9.3
I3d	621.37	1.29	34775.78	2.92

Name	Peak BE	FWHM eV	Area (P) CPS.eV	Weight %
C1s	285.69	1.79	180184.44	45.74
O1s	532.4	1.87	149575.16	20.92
S2p	168.55	3.78	52620.83	17.65
F1s	688.59	1.82	96142.83	12.77
I3d	621.37	1.32	35909.27	2.91

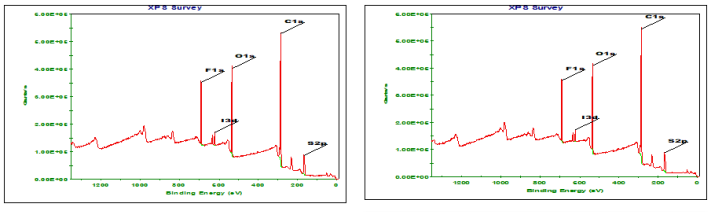

Name	Peak BE	FWHM eV	Area (P) CPS.eV	Weight %
C1s	285.6	1.78	184221.9	46.26
O1s	532.37	1.95	150924.76	20.88
S2p	168.53	3.78	52358.92	17.37
F1s	688.55	1.82	95079.64	12.49
I3d	621.3	1.29	37453.92	3

Name	Peak BE	FWHM eV	Area (P) CPS.eV	Weight %
C1s	285.61	1.77	190446.97	47.01
O1s	532.45	2.61	153441.75	20.87
S2p	168.52	3.85	53157.77	17.33
F1s	688.58	1.84	93044.88	12.02
I3d	621.32	1.31	35175.11	2.77

Figure S6: XPS spectrum of polymer **3b**

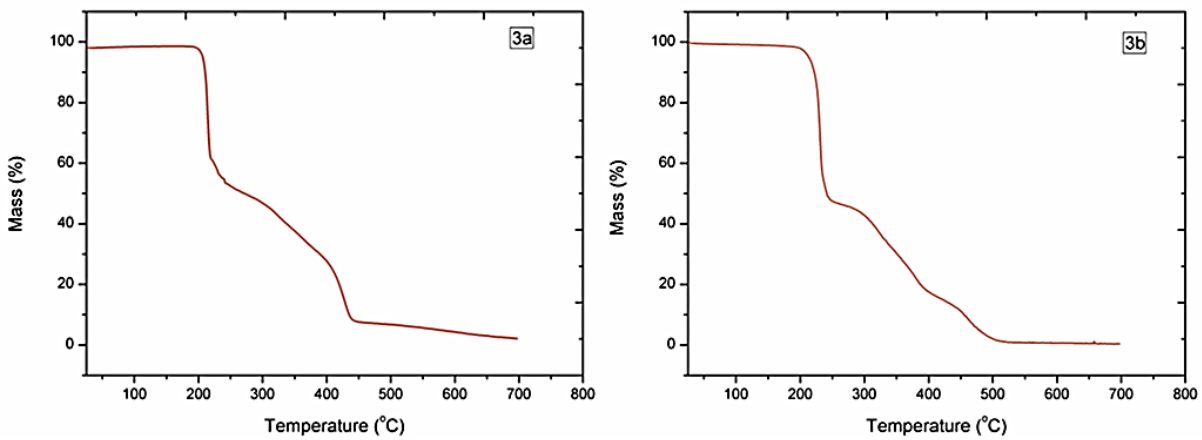

Figure S7: TGA graph of polymer **3a** and **3b**

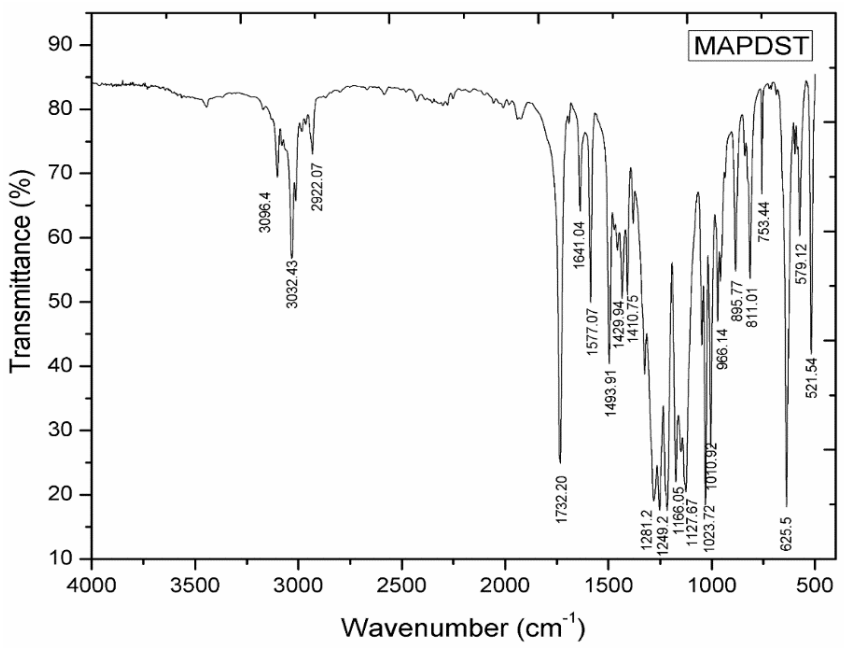

Figure S8: FTIR spectrum of 4-(methacryloyloxy)phenyl dimethylsulfonium triflate (MAPDST)

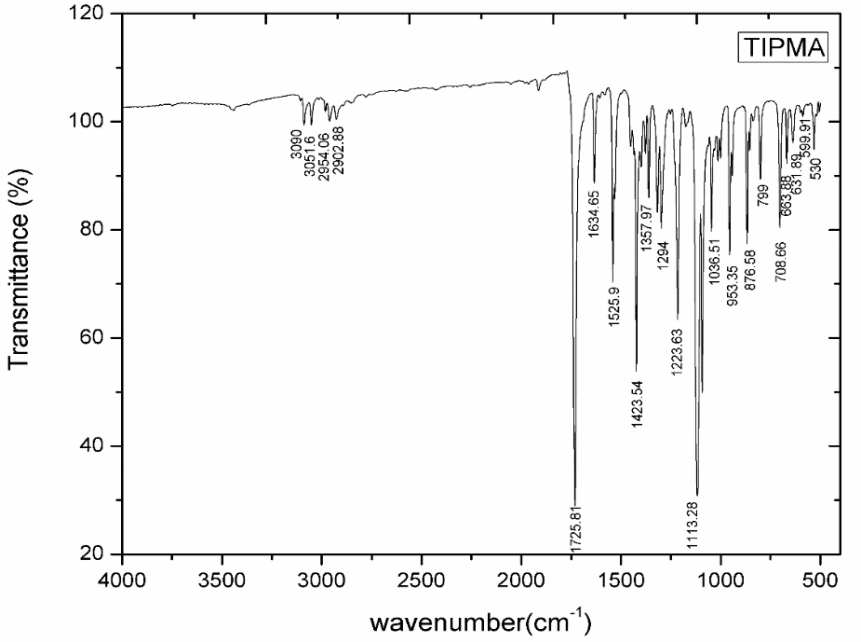

Figure S9: FTIR spectrum of 2,4,6-triiodophenyl methacrylate (TIPMA)

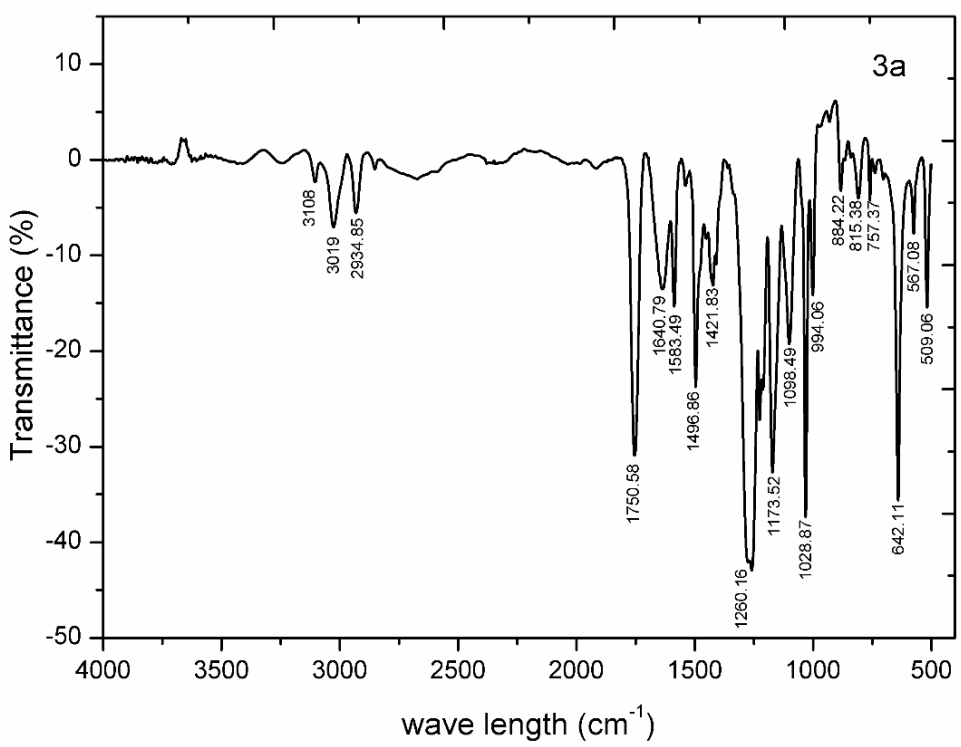

Figure S10: FTIR spectrum of polymer **3a**

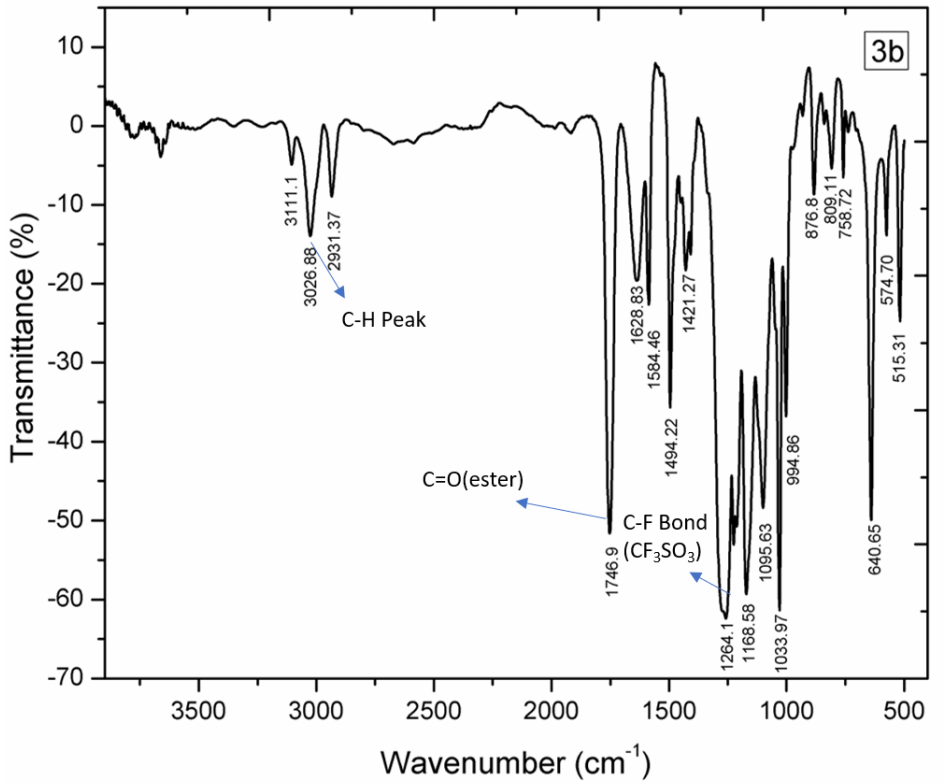

Figure S11: FTIR spectrum of polymer **3b**

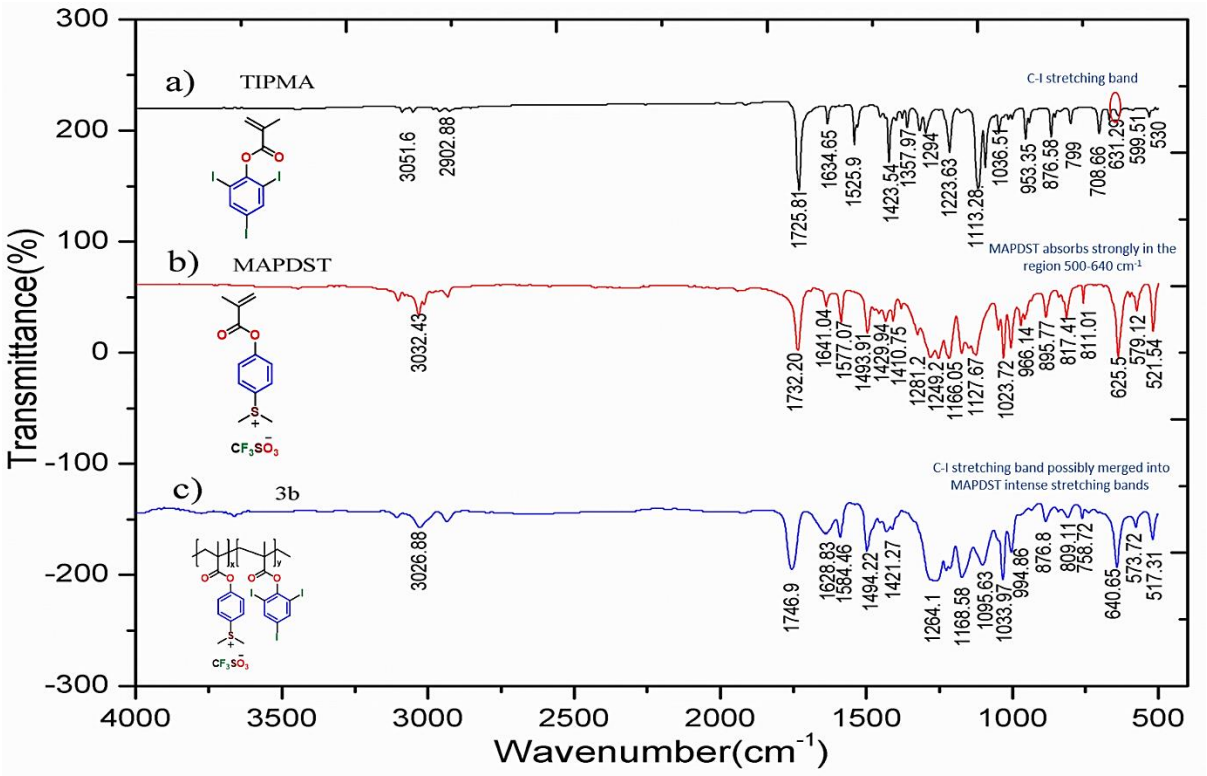

Figure S12: Stacked FTIR spectrum of TIPMA, MAPDST and polymer **3b**

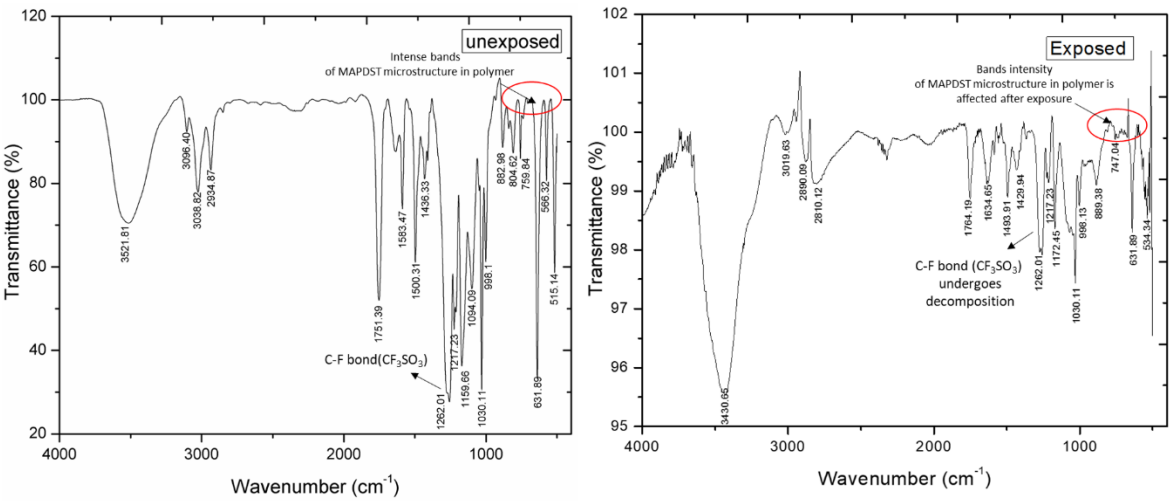

Figure S13: FTIR spectrum of exposed and unexposed polymer **3b**

Note: The OH stretching peak in both cases (exposed and unexposed) is due to the presence of residual methanol as the resist films were stripped off from silicon surface using methanol.

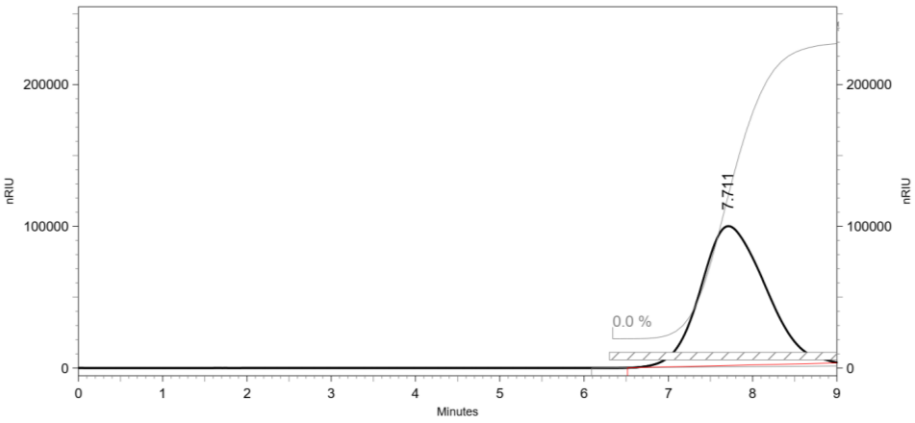

SEC Summary information

RID: RI Signal	
Processing Start Time(min)	6.300
Processing Stop Time(min)	9.200
Number of Slices	34
Weight Average Molecular Weight	10694
Number Average Molecular Weight	5144
Z Average Molecular Weight	19121
Z+1 Average Molecular Weight	33551
Polydispersity index	2.079
Peak Molecular Weight	8479
Z Average / Weight Average	1.788
Z+1 Average / Weight Average	3.137

Figure S14: GPC graph of polymer **3a**

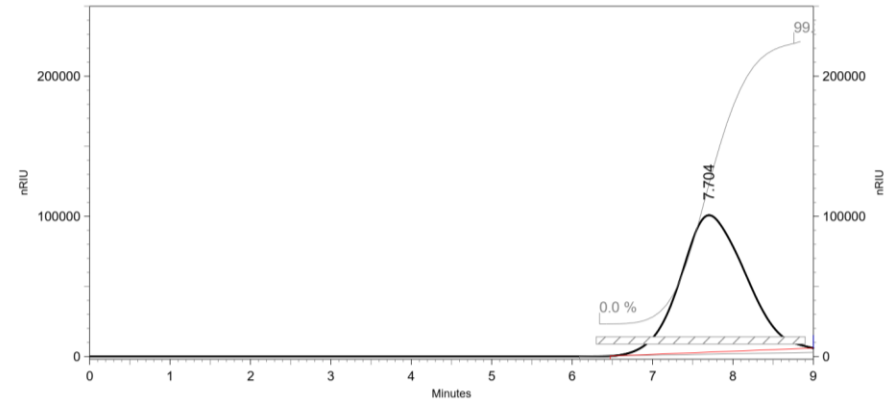

SEC Summary information

RID: RI Signal	
Processing Start Time(min)	6.300
Processing Stop Time(min)	8.900
Number of Slices	31
Weight Average Molecular Weight	11780
Number Average Molecular Weight	5469
Z Average Molecular Weight	22794
Z+1 Average Molecular Weight	40687
Polydispersity index	2.154
Peak Molecular Weight	8619
Z Average / Weight Average	1.935
Z+1 Average / Weight Average	3.454

Figure S15: GPC graph of polymer **3b**

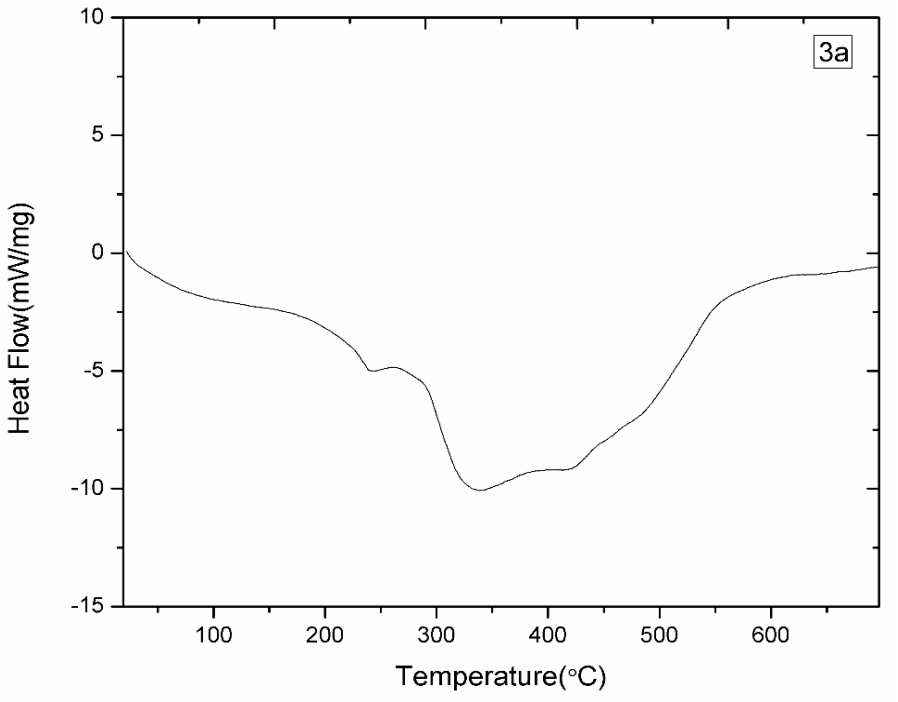

Figure S16: DSC graph of polymer **3a**

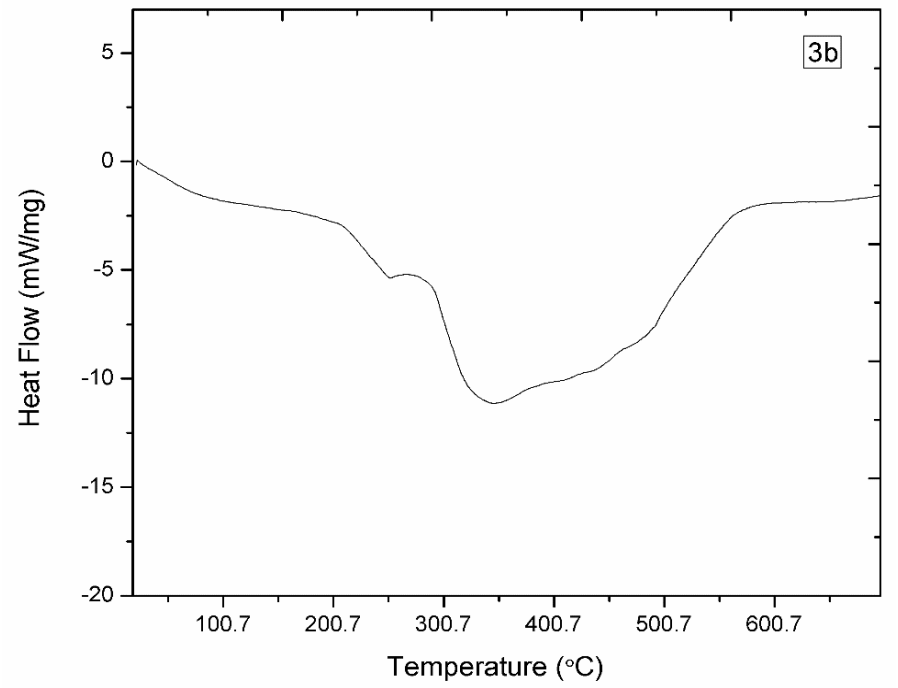

Figure S17: DSC graph of polymer **3b**

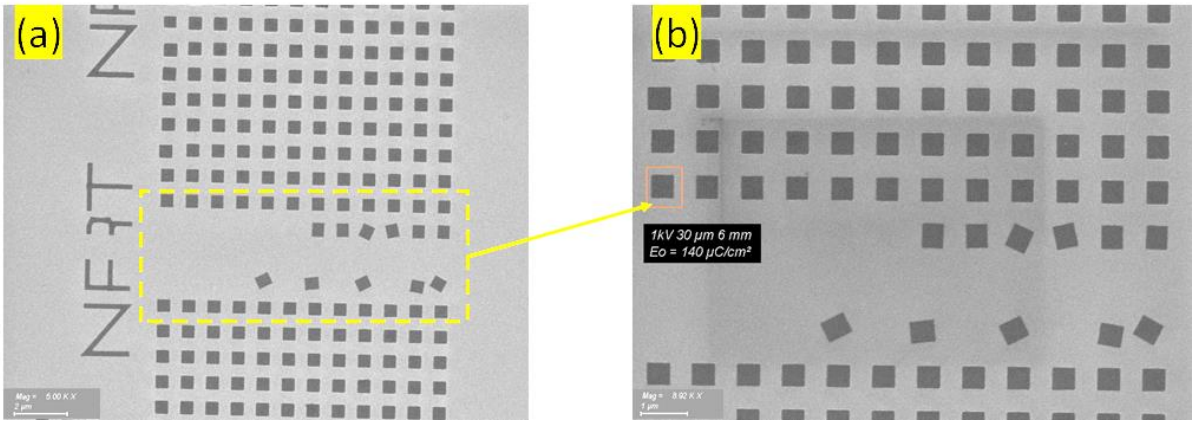

Figure S18: SEM micrograph of patterned **3b** with 1 keV beam energy; the result shows the delocalised fully patterned resist on Si substrate.

The modelled trajectory of 1 keV e-beam inside 40 nm Resist/Si under CASINO 2.48. The detailed simulation process has been discussed by Moinuddin *et al.*[3]

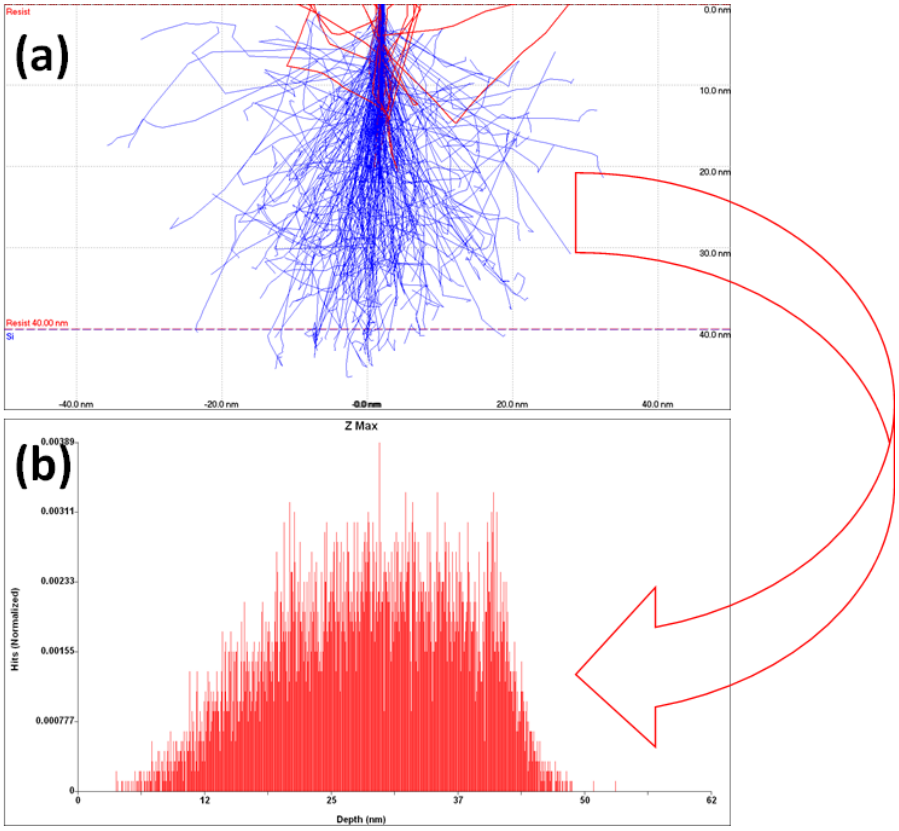

Figure S19: Conceptualization of stopping power for 1 keV and pattern damage analysis under Monte Carlo simulation using Casino tool. (a) 1 keV e-beam trajectory showcase with a resist thickness of 40 nm. (b) Probabilistic distribution of electron traveling inside the resist with 1 keV.

Figure **S19** shows the modelled beam inside the resist and their traveling trajectories. Figure 19(a) suggests that at a critical dose (Eo) 1keV beam cannot travel completely inside the resist. Beyond the critical limit, the localized energy transport due to the e-beam may be the possible mechanism for stable exposure at 1 keV. It also suggests that energy deposited inside the resist is completely consumed by resist hence low dose is required. Figure **S19b** shows the probabilistic distribution of e-beam inside the resist when exposed with 1 keV.[3,4]

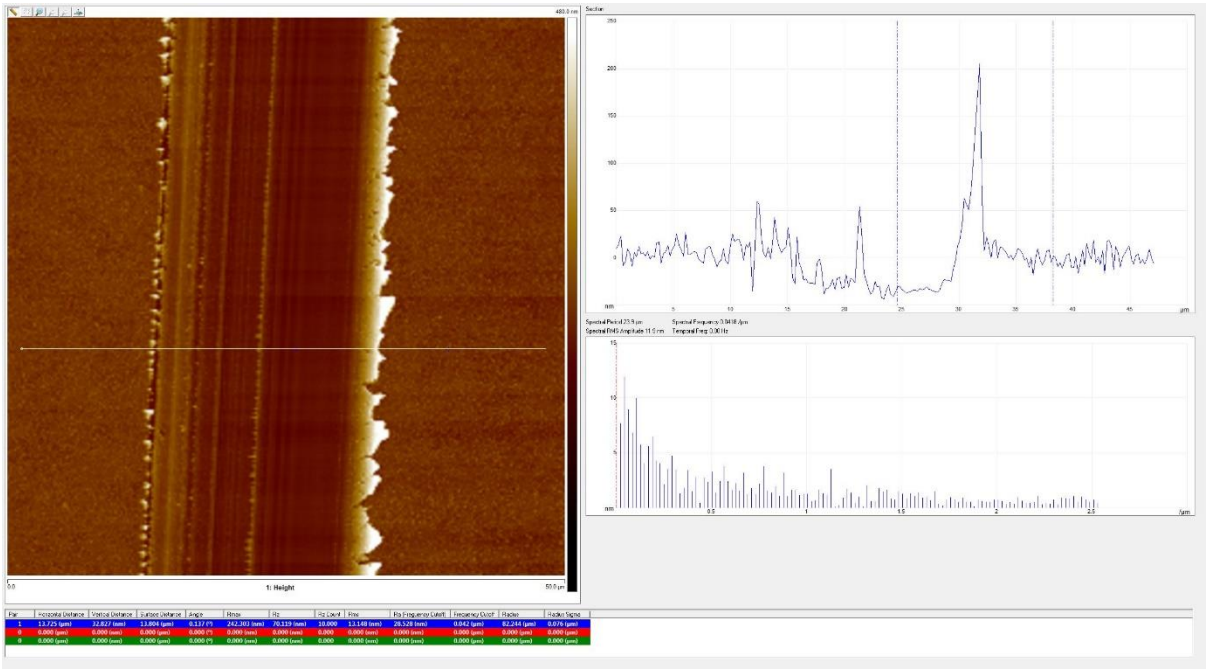

Figure S20: Resist thickness measurement using AFM (33 nm)

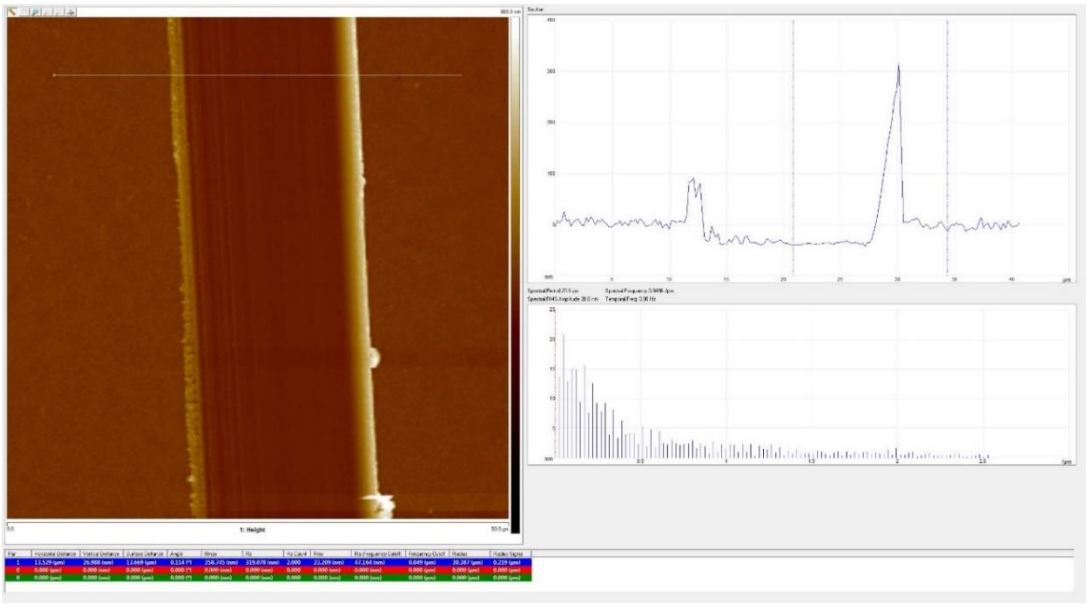

Figure S21: Resist thickness measurement using AFM (27 nm)

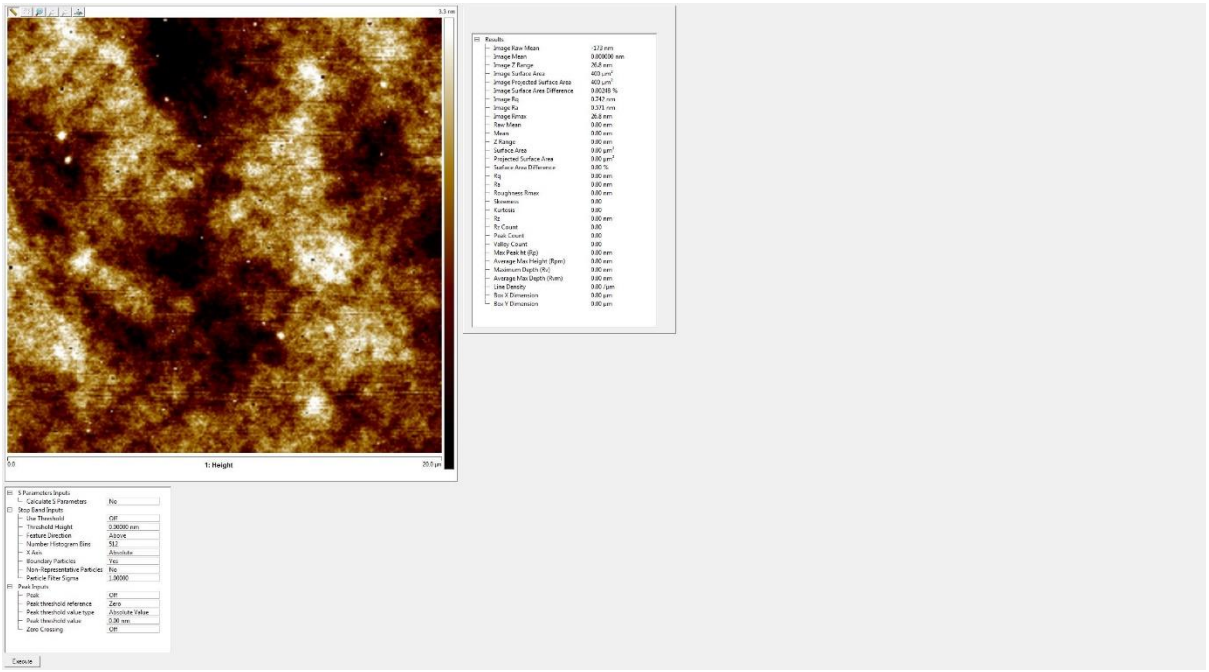

Figure S22: Roughness measurement using AFM (Rq = 0.742)

While analysing the LER/LWR data, the shot or raster scan noise might influence the actual information. The presence of any noise during imaging may lead to the degradation of the image as well as the raw information (edge roughness).[5] Shot noise predominantly plays a key role while imaging the nanostructures. Hence, protecting the edges and structural details of nanopatterns along with noise reduction is the main challenge of noise-reduction filters.[5]

To avoid the raster noise, images were taken with 1024 x 768 pixels at 100k magnification i.e ~1.0 nm/pixel (see Figure S23a). Wiener filtering was adapted to enhance the image quality affected by shot noise, and hence the possible information from the image could be restored.[6]. Further, Wiener filtering was convoluted on imaged patterns and smoothed data are shown in Figure S23b.

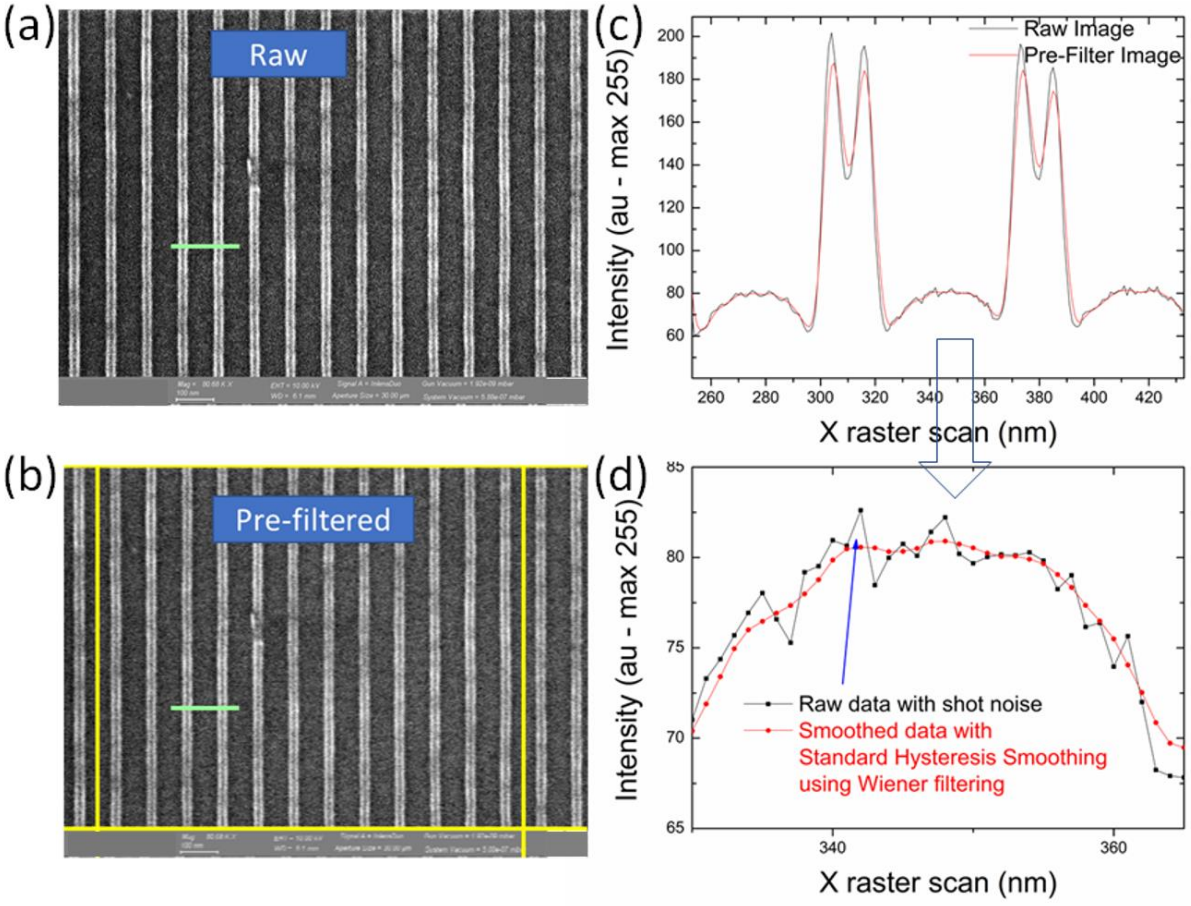

Figure S23: Image pattern and noise cancelation analysis for LER/LWR. (a) Raw image of captured 20 nm line patterns from 20 keV e-beam. (b) Pre-filtered SEM image of nano-patterns. (c) Intensity spectra of line patterns for with and without pre-filter image processing. (d) Smoothed data with standard hysteresis smoothing using Wiener filters.

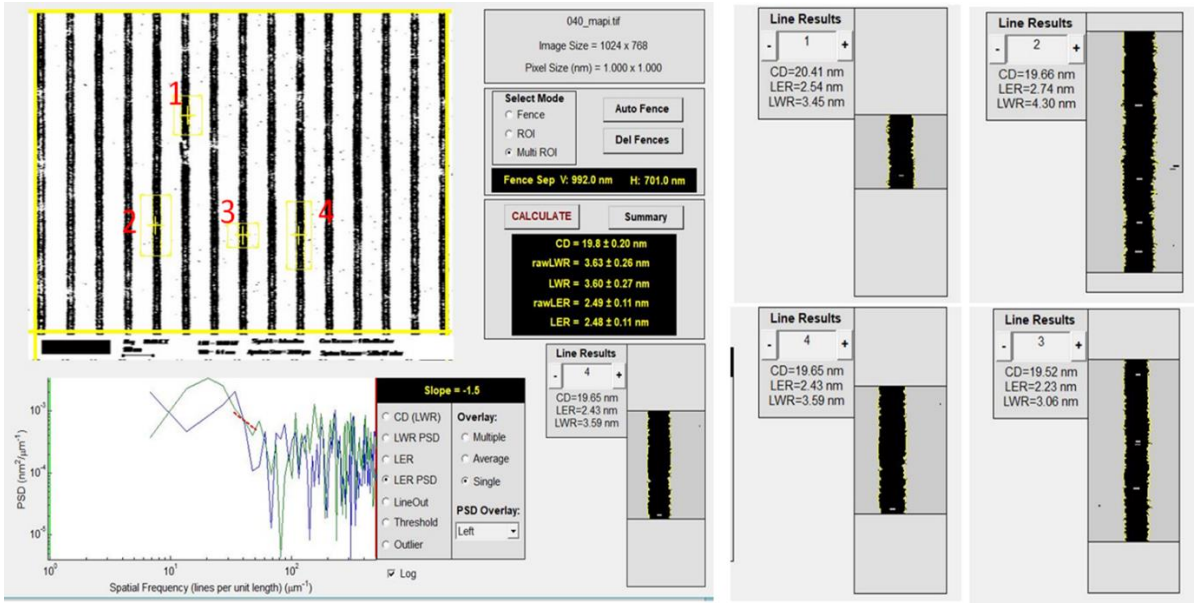

Figure S24: Computed LER/LWR values from prefiltered patterns under threshold condition. Different line results depict the different region of interest as mentioned in pattern image (1, 2, 3 and 4).

Mole percentage calculation:

For polymer microstructure calculation initially iodine percentage was analysed from XPS data. For this purpose, five sets of samples were prepared (for each polymer) and the average of iodine percentage of five sets was considered for further calculation. Similarly, the weight average molecular weight (Mw) of the individual polymer was calculated from gel permeation chromatography (GPC) analysis. With the help of iodine percentage and molecular weight, the total iodine content was evaluated. The total iodine content was used to calculate the total TIPMA content, which was further used to calculate mole fraction of TIPMA. The subtractions of TIPMA from molecular weight gave the total MAPDST content which was used further to calculate MAPDST mole fraction. These two mole fractions gave the microstructure composition.

The detailed mathematical calculation is given below.

Microstructure calculation for 3a

Average iodine (%) calculated From XPS data

S.no	XPS Data 3a	
1	1.88	
2	1.99	
3	1.82	
4	1.83	
5	1.9	Average
Total	9.42	1.88

Molecular weight of MAPDST (a) = 372

Molecular weight of TIPMA (b) = 539.76

Atomic weight of iodine (c) = 126.9

Percentage of iodine obtained from XPS (d) = 1.88% = 0.0188

Molecular weight of co-polymer obtained from GPC (e) = 10694

Total iodine content present in the polymer (f)= e*d

= 201.04

Total TIPMA amount present in the polymer (g) = b*f/c

= 855.13

No of mmoles of TIPMA (h) = g/b

= 1.58

Total MAPDST amount present in the polymer (i) = e-g

= 9838.86

No of mmoles of MAPDST (j) = i/a

= 26.44

∴The Ratio of MAPDST: TIPMA = 26.44: 1.58

Monomers	Microstructure (%)
MAPDST	94.3
TIPMA	5.7

Microstructure calculation for polymer 3b

Average iodine (%) calculated From XPS data

S.no	XPS Data 3b	
1	2.95	
2	2.92	
3	2.91	
4	3	
5	2.77	Average
Total	14.55	2.91

Molecular weight of MAPDST (a) = 372

Molecular weight of TIPMA (b) = 539.76

Atomic weight of iodine (c) = 126.9

Percentage of iodine obtained from XPS (d) = 2.91% = 0.0291

Molecular weight of co-polymer obtained from GPC (e)= 11780

Total iodine content present in the polymer (f) = e * d

= 342.8

Total TIPMA amount present in the polymer (g) = b * f /c

= 1458.06

No of mmoles of TIPMA (h) = g/b

= 2.7

Total MAPDST amount present in the polymer (i) = e-g

= 10321.93

No of mmoles of MAPDST (j) = i/a

= 27.74

∴Ratio of MAPDST: TIPMA = 27.74: 2.7

Monomers	Microstructure (%)
MAPDST	91.1
TIPMA	8.9

References

(1) Satyanarayana, V. S. V.; Kessler, F.; Singh, V.; Scheffer, F. R.; Weibel, D. E.; Ghosh, S.; Gonsalves, K. E. Radiation-Sensitive Novel Polymeric Resist Materials: Iterative Synthesis and Their EUV Fragmentation Studies. ACS Appl. Mater. Interfaces 2014, 6 (6), 4223–4232. https://doi.org/10.1021/am405905p.

(2) Wang, Z.; Chang, T.; Hunter, L.; Gregory, A. M.; Tanudji, M.; Jones, S.; Stenzel, M. H. Radio-Opaque Micelles for X-Ray Imaging. Aust. J. Chem. 2014, 67 (1), 78–84. https://doi.org/10.1071/CH13391.

(3) Moinuddin, M. G.; Kumar, R.; Yogesh, M.; Sharma, S.; Sahani, M.; Sharma, S. K.; Gonsalves, K. E. Functionalized Ag Nanoparticles Embedded in Polymer Resists for High-Resolution Lithography. *ACS Appl. Nano Mater.* **2020**, *3* (9), 8651–8661. https://doi.org/10.1021/acsanm.0c01362.

(4) Kyser, D. F.; Viswanathan, N. S. Monte Carlo Simulation of Spatially Distributed Beams in Electron-Beam Lithography. *J Vac Sci Technol* **1975**, *12* (6), 1305–1308. https://doi.org/10.1116/1.568524.

(5) Mazhari, M. and Hasanzadeh, R.P.R., Suppression of noise in SEM images using weighted local hysteresis smoothing filter. Scanning, **2016**, *38*, 634-643. https://doi.org/10.1002/sca.21311.

(6) Sim, K.S., Teh, V. and Nia, M.E. (2016), Adaptive noise Wiener filter for scanning electron microscope imaging system. Scanning, **2016**, *38*, 148-163. https://doi.org/10.1002/sca.21250.